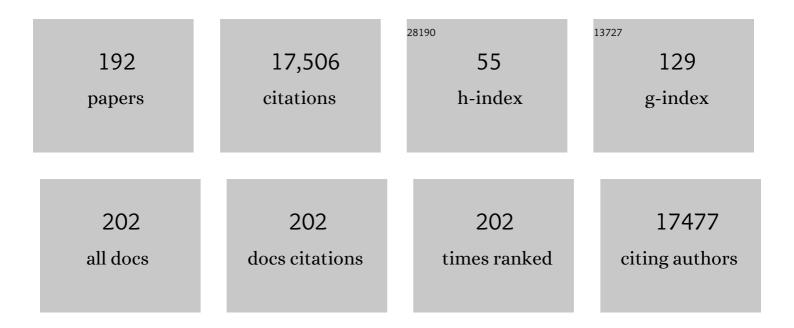
List of Publications by Year in descending order

Source: https://exaly.com/author-pdf/3023137/publications.pdf Version: 2024-02-01



#	Article	IF	CITATIONS
1	The structure of NLRP9 reveals a unique Câ€ŧerminal region with putative regulatory function. FEBS Letters, 2022, 596, 876-885.	1.3	4
2	A crystal-processing machine using a deep-ultraviolet laser: application to long-wavelength native SAD experiments. Acta Crystallographica Section F, Structural Biology Communications, 2022, 78, 88-95.	0.4	1
3	Comparison of six antibody assays and two combination assays for COVID-19. Virology Journal, 2022, 19, 24.	1.4	5
4	Structureâ€based engineering of a shortâ€chain <i>cis</i> â€prenyltransferase to biosynthesize nonnatural allâ€ <i>cis</i> â€polyisoprenoids: molecular mechanisms for primer substrate recognition and ultimate product chainâ€length determination. FEBS Journal, 2022, 289, 4602-4621.	2.2	4
5	Macromolecular Crystallography at SPring-8. Nihon Kessho Gakkaishi, 2022, 64, 2-9.	0.0	Ο
6	<i>In situ</i> crystal data-collection and ligand-screening system at SPring-8. Acta Crystallographica Section F, Structural Biology Communications, 2022, 78, 241-251.	0.4	7
7	Crystal structure of chalcone synthase, a key enzyme for isoflavonoid biosynthesis in soybean. Proteins: Structure, Function and Bioinformatics, 2021, 89, 126-131.	1.5	6
8	Cryo-EM Structure of the Prostaglandin E Receptor EP4 Coupled to G Protein. Structure, 2021, 29, 252-260.e6.	1.6	32
9	An unprecedented insight into the catalytic mechanism of copper nitrite reductase from atomic-resolution and damage-free structures. Science Advances, 2021, 7, .	4.7	25
10	Evaluation of the data-collection strategy for room-temperature micro-crystallography studied by serial synchrotron rotation crystallography combined with the humid air and glue-coating method. Acta Crystallographica Section D: Structural Biology, 2021, 77, 300-312.	1.1	7
11	Comparison of 12 Molecular Detection Assays for Severe Acute Respiratory Syndrome Coronavirus 2 (SARS-CoV-2). Journal of Molecular Diagnostics, 2021, 23, 164-170.	1.2	29
12	Common architectures in cyanobacteria Prochlorococcus cells visualized by X-ray diffraction imaging using X-ray free electron laser. Scientific Reports, 2021, 11, 3877.	1.6	8
13	XFEL Crystal Structures of Peroxidase Compound II. Angewandte Chemie - International Edition, 2021, 60, 14578-14585.	7.2	18
14	XFEL Crystal Structures of Peroxidase Compound II. Angewandte Chemie, 2021, 133, 14699-14706.	1.6	0
15	Short-lived intermediate in N ₂ O generation by P450 NO reductase captured by time-resolved IR spectroscopy and XFEL crystallography. Proceedings of the National Academy of Sciences of the United States of America, 2021, 118, .	3.3	21
16	Guidelines for <i>de novo</i> phasing using multiple small-wedge data collection. Journal of Synchrotron Radiation, 2021, 28, 1284-1295.	1.0	7
17	Structural Basis for the Binding Mechanism of Human Serum Albumin Complexed with Cyclic Peptide Dalbavancin. Journal of Medicinal Chemistry, 2020, 63, 14045-14053.	2.9	13
18	Human adiponectin receptor AdipoR1 assumes closed and open structures. Communications Biology, 2020. 3. 446.	2.0	15

#	Article	IF	CITATIONS
19	Room-temperature crystallography using a microfluidic protein crystal array device and its application to protein–ligand complex structure analysis. Chemical Science, 2020, 11, 9072-9087.	3.7	18
20	Isoprenoid-chained lipid EROCOC17+4: a new matrix for membrane protein crystallization and a crystal delivery medium in serial femtosecond crystallography. Scientific Reports, 2020, 10, 19305.	1.6	16
21	Methods and application of coherent X-ray diffraction imaging of noncrystalline particles. Biophysical Reviews, 2020, 12, 541-567.	1.5	16
22	Crystal structure of pathogenic Staphylococcus aureus lipase complex with the anti-obesity drug orlistat. Scientific Reports, 2020, 10, 5469.	1.6	16
23	Computer-controlled liquid-nitrogen drizzling device for removing frost from cryopreserved crystals. Acta Crystallographica Section F, Structural Biology Communications, 2020, 76, 616-622.	0.4	5
24	Development of SPACE-II for rapid sample exchange at SPring-8 macromolecular crystallography beamlines. Acta Crystallographica Section D: Structural Biology, 2020, 76, 155-165.	1.1	12
25	Catalytically important damage-free structures of a copper nitrite reductase obtained by femtosecond X-ray laser and room-temperature neutron crystallography. IUCrJ, 2019, 6, 761-772.	1.0	24
26	Phagocytosis is mediated by two-dimensional assemblies of the F-BAR protein GAS7. Nature Communications, 2019, 10, 4763.	5.8	31
27	An oxyl/oxo mechanism for oxygen-oxygen coupling in PSII revealed by an x-ray free-electron laser. Science, 2019, 366, 334-338.	6.0	248
28	Upgrade of bending magnet MX beamline BL38B1 at SPring-8. AIP Conference Proceedings, 2019, , .	0.3	0
29	Dimeric structures of quinol-dependent nitric oxide reductases (qNORs) revealed by cryo–electron microscopy. Science Advances, 2019, 5, eaax1803.	4.7	14
30	<i>In crystallo</i> thermodynamic analysis of conformational change of the topaquinone cofactor in bacterial copper amine oxidase. Proceedings of the National Academy of Sciences of the United States of America, 2019, 116, 135-140.	3.3	10
31	Ligand binding to human prostaglandin E receptor EP4 at the lipid-bilayer interface. Nature Chemical Biology, 2019, 15, 18-26.	3.9	85
32	Crystal structure of the endogenous agonist-bound prostanoid receptor EP3. Nature Chemical Biology, 2019, 15, 8-10.	3.9	49
33	A temperature-controlled cold-gas humidifier and its application to protein crystals with the humid-air and glue-coating method. Journal of Applied Crystallography, 2019, 52, 699-705.	1.9	9
34	DeepCentering: fully automated crystal centering using deep learning for macromolecular crystallography. Journal of Synchrotron Radiation, 2019, 26, 1361-1366.	1.0	18
35	Low-dose X-ray structure analysis of cytochrome <i>c</i> oxidase utilizing high-energy X-rays. Journal of Synchrotron Radiation, 2019, 26, 912-921.	1.0	16
36	Long-wavelength native-SAD phasing: opportunities and challenges. IUCrJ, 2019, 6, 373-386.	1.0	22

#	Article	IF	CITATIONS
37	<i>ZOO</i> : an automatic data-collection system for high-throughput structure analysis in protein microcrystallography. Acta Crystallographica Section D: Structural Biology, 2019, 75, 138-150.	1.1	156
38	Data Collection Strategy in Protein Micro-crystallography at Synchrotron Facility. Seibutsu Butsuri, 2019, 59, 215-218.	0.0	0
39	Remodeling of the optics for a micro-focusing protein crystallography beamline at SPring-8. , 2019, , .		0
40	Architecture of the complete oxygen-sensing FixL-FixJ two-component signal transduction system. Science Signaling, 2018, 11, .	1.6	38
41	Shot-by-shot characterization of focused X-ray free electron laser pulses. Scientific Reports, 2018, 8, 831.	1.6	20
42	Blue light–excited LOV1 and LOV2 domains cooperatively regulate the kinase activity of full-length phototropin2 from Arabidopsis. Journal of Biological Chemistry, 2018, 293, 963-972.	1.6	17
43	Na+-mimicking ligands stabilize the inactive state of leukotriene B4 receptor BLT1. Nature Chemical Biology, 2018, 14, 262-269.	3.9	80
44	Crystal Structures of Human Orexin 2 Receptor Bound to the Subtype-Selective Antagonist EMPA. Structure, 2018, 26, 7-19.e5.	1.6	55
45	Structural insights into the subtype-selective antagonist binding to the M2 muscarinic receptor. Nature Chemical Biology, 2018, 14, 1150-1158.	3.9	59
46	Cryogenic Coherent X-ray Diffraction Imaging Techniques for Structural Analyses of Biological Cells and Cellular Organelles. Microscopy and Microanalysis, 2018, 24, 14-15.	0.2	0
47	Molecular Analysis of a <i>bla</i> _{IMP-1} -Harboring Class 3 Integron in Multidrug-Resistant Pseudomonas fulva. Antimicrobial Agents and Chemotherapy, 2018, 62, .	1.4	5
48	Diffraction apparatus and procedure in tomography X-ray diffraction imaging for biological cells at cryogenic temperature using synchrotron X-ray radiation. Journal of Synchrotron Radiation, 2018, 25, 1803-1818.	1.0	10
49	An unprecedented dioxygen species revealed by serial femtosecond rotation crystallography in copper nitrite reductase. IUCrJ, 2018, 5, 22-31.	1.0	27
50	<i>KAMO</i> : towards automated data processing for microcrystals. Acta Crystallographica Section D: Structural Biology, 2018, 74, 441-449.	1.1	198
51	Crystal structure of a family 80 chitosanase from <i>Mitsuaria chitosanitabida</i> . FEBS Letters, 2017, 591, 540-547.	1.3	22
52	Light-induced structural changes and the site of O=O bond formation in PSII caught by XFEL. Nature, 2017, 543, 131-135.	13.7	515
53	Structural basis for ligand capture and release by the endocytic receptor Apo ER 2. EMBO Reports, 2017, 18, 982-999.	2.0	26
54	Development of a dose-limiting data collection strategy for serial synchrotron rotation crystallography. Journal of Synchrotron Radiation, 2017, 24, 29-41.	1.0	39

#	Article	IF	CITATIONS
55	A nanosecond time-resolved XFEL analysis of structural changes associated with CO release from cytochrome c oxidase. Science Advances, 2017, 3, e1603042.	4.7	68
56	Capturing an initial intermediate during the P450nor enzymatic reaction using time-resolved XFEL crystallography and caged-substrate. Nature Communications, 2017, 8, 1585.	5.8	74
57	Common structural features of toxic intermediates from α-synuclein and GroES fibrillogenesis detected using cryogenic coherent X-ray diffraction imaging. Journal of Biochemistry, 2017, 161, 55-65.	0.9	8
58	Protein microcrystallography using synchrotron radiation. IUCrJ, 2017, 4, 529-539.	1.0	56
59	Experimental phase determination with selenomethionine or mercury-derivatization in serial femtosecond crystallography. IUCrJ, 2017, 4, 639-647.	1.0	24
60	Coherent X-ray Diffraction Imaging of Cyanidioschyzon merolae. , 2017, , 153-173.		0
61	A nearly on-axis spectroscopic system for simultaneouslyÂmeasuring UV–visible absorption and X-ray diffraction in the SPring-8 structural genomics beamline. Journal of Synchrotron Radiation, 2016, 23, 334-338.	1.0	4
62	SPring-8 BL44XU, beamline designed for structure analysis of large biological macromolecular assemblies. AIP Conference Proceedings, 2016, , .	0.3	6
63	Remote access and automation of SPring-8 MX beamlines. AIP Conference Proceedings, 2016, , .	0.3	23
64	Interspecies Dissemination of a Mobilizable Plasmid Harboring <i>bla</i> _{IMP-19} and the Possibility of Horizontal Gene Transfer in a Single Patient. Antimicrobial Agents and Chemotherapy, 2016, 60, 5412-5419.	1.4	17
65	Molecular Mechanism for Conformational Dynamics of Ras·GTP Elucidated from In-Situ Structural Transition in Crystal. Scientific Reports, 2016, 6, 25931.	1.6	42
66	TAKASAGO-6 apparatus for cryogenic coherent X-ray diffraction imaging of biological non-crystalline particles using X-ray free electron laser at SACLA. Review of Scientific Instruments, 2016, 87, 053109.	0.6	27
67	X-ray Crystallographic Structure of Thermophilic Rhodopsin. Journal of Biological Chemistry, 2016, 291, 12223-12232.	1.6	38
68	Specimen preparation for cryogenic coherent X-ray diffraction imaging of biological cells and cellular organelles by using the X-ray free-electron laser at SACLA. Journal of Synchrotron Radiation, 2016, 23, 975-989.	1.0	38
69	Blue Light-excited Light-Oxygen-Voltage-sensing Domain 2 (LOV2) Triggers a Rearrangement of the Kinase Domain to Induce Phosphorylation Activity in Arabidopsis Phototropin1. Journal of Biological Chemistry, 2016, 291, 19975-19984.	1.6	10
70	Taste substance binding elicits conformational change of taste receptor T1r heterodimer extracellular domains. Scientific Reports, 2016, 6, 25745.	1.6	36
71	Cell-free methods to produce structurally intact mammalian membrane proteins. Scientific Reports, 2016, 6, 30442.	1.6	56
72	Structural basis for disruption of claudin assembly in tight junctions by an enterotoxin. Scientific Reports, 2016, 6, 33632.	1.6	85

#	Article	IF	CITATIONS
73	Radiation Damage-Free Structure of Photosystem II Determined by Femtosecond X-Ray Free Electron Laser Pulses. Nihon Kessho Gakkaishi, 2016, 58, 126-132.	0.0	1
74	An isomorphous replacement method for efficient de novo phasing for serial femtosecond crystallography. Scientific Reports, 2015, 5, 14017.	1.6	54
75	Determination of Damage-free Crystal Structure of an X-ray Sensitive Protein Using XFEL. Nihon Kessho Gakkaishi, 2015, 57, 122-128.	0.0	158
76	Crystal Structure of OXA-58 with the Substrate-Binding Cleft in a Closed State: Insights into the Mobility and Stability of the OXA-58 Structure. PLoS ONE, 2015, 10, e0145869.	1.1	7
77	Coherent X-Ray Diffraction Imaging of Chloroplasts from <i>Cyanidioschyzon merolae</i> by Using X-Ray Free Electron Laser. Plant and Cell Physiology, 2015, 56, 1272-1286.	1.5	56
78	Expression, purification, crystallization, and preliminary X-ray crystallographic studies of the human adiponectin receptors, AdipoR1 and AdipoR2. Journal of Structural and Functional Genomics, 2015, 16, 11-23.	1.2	14
79	A Novel Allosteric Mechanism on Protein–DNA Interactions underlying the Phosphorylation-Dependent Regulation of Ets1 Target Gene Expressions. Journal of Molecular Biology, 2015, 427, 1655-1669.	2.0	22
80	Molecular basis of ligand recognition and transport by glucose transporters. Nature, 2015, 526, 391-396.	13.7	305
81	Structure of the RsbX phosphatase involved in the general stress response of <i>Bacillus subtilis</i> . Acta Crystallographica Section D: Biological Crystallography, 2015, 71, 1392-1399.	2.5	8
82	A magnetic anti-cancer compound for magnet-guided delivery and magnetic resonance imaging. Scientific Reports, 2015, 5, 9194.	1.6	40
83	Small-angle X-ray scattering analysis reveals the ATP-bound monomeric state of the ATPase domain from the homodimeric MutL endonuclease, a CHKL phosphotransferase superfamily protein. Extremophiles, 2015, 19, 643-656.	0.9	6
84	Crystal structures of the human adiponectin receptors. Nature, 2015, 520, 312-316.	13.7	176
85	Cryogenic coherent x-ray diffraction imaging for biological non-crystalline particles using the KOTOBUKI-1 diffraction apparatus at SACLA. Journal of Physics B: Atomic, Molecular and Optical Physics, 2015, 48, 184003.	0.6	32
86	Native structure of photosystem II at 1.95ÂÃ resolution viewed by femtosecond X-ray pulses. Nature, 2015, 517, 99-103.	13.7	1,050
87	Changes in Surgical Site Infections after Living Donor Liver Transplantation. PLoS ONE, 2015, 10, e0136559.	1.1	17
88	Crystal structure of a bacterial homologue of SWEET transporters. Cell Research, 2014, 24, 1486-1489.	5.7	71
89	Light-induced Conformational Changes of LOV1 (Light Oxygen Voltage-sensing Domain 1) and LOV2 Relative to the Kinase Domain and Regulation of Kinase Activity in Chlamydomonas Phototropin. Journal of Biological Chemistry, 2014, 289, 413-422.	1.6	40
90	Determination of damage-free crystal structure of an X-ray–sensitive protein using an XFEL. Nature Methods, 2014, 11, 734-736.	9.0	237

#	Article	IF	CITATIONS
91	Single-shot three-dimensional structure determination of nanocrystals with femtosecond X-ray free-electron laser pulses. Nature Communications, 2014, 5, 4061.	5.8	91
92	<i>IDATEN</i> and <i>G-SITENNO</i> : GUI-assisted software for coherent X-ray diffraction imaging experiments and data analyses at SACLA. Journal of Synchrotron Radiation, 2014, 21, 1378-1383.	1.0	18
93	Current status of protein micro-crystallography at SPring-8. Acta Crystallographica Section A: Foundations and Advances, 2014, 70, C333-C333.	0.0	1
94	Clinical characteristics and risk factors of non-Candida fungaemia. BMC Infectious Diseases, 2013, 13, 247.	1.3	20
95	Coherent Diffraction Imaging Analysis of Shape-Controlled Nanoparticles with Focused Hard X-ray Free-Electron Laser Pulses. Nano Letters, 2013, 13, 6028-6032.	4.5	57
96	Achievement of protein micro-crystallography at SPring-8 beamline BL32XU. Journal of Physics: Conference Series, 2013, 425, 012002.	0.3	72
97	Molecular dissection of IZUMO1, a sperm protein essential for sperm-egg fusion. Development (Cambridge), 2013, 140, 3221-3229.	1.2	102
98	Sagittal focusing of synchrotron radiation X-rays using a winged crystal. Journal of Synchrotron Radiation, 2013, 20, 219-225.	1.0	14
99	SPring-8 BL41XU, a high-flux macromolecular crystallography beamline. Journal of Synchrotron Radiation, 2013, 20, 910-913.	1.0	25
100	Development of an online UV–visible microspectrophotometer for a macromolecular crystallography beamline. Journal of Synchrotron Radiation, 2013, 20, 948-952.	1.0	10
101	KOTOBUKI-1 apparatus for cryogenic coherent X-ray diffraction imaging. Review of Scientific Instruments, 2013, 84, 093705.	0.6	51
102	<i>In silico</i> discovery of small-molecule Ras inhibitors that display antitumor activity by blocking the Ras–effector interaction. Proceedings of the National Academy of Sciences of the United States of America, 2013, 110, 8182-8187.	3.3	272
103	Tracking X-ray microscopy for alveolar dynamics in live intact mice. Scientific Reports, 2013, 3, 1304.	1.6	12
104	Post-Transcriptional Regulator Hfq Binds Catalase HPII: Crystal Structure of the Complex. PLoS ONE, 2013, 8, e78216.	1.1	8
105	Abstract 5570: Targeted drug delivery system and magnetic resonance imaging with intrinsic ferromagnetic nano-particle compound , 2013, , .		0
106	Fast microtomography using bright monochromatic x-rays. Review of Scientific Instruments, 2012, 83, 093704.	0.6	13
107	Molecular characterization of IMP-type metallo-Â-lactamases among multidrug-resistant Achromobacter xylosoxidans. Journal of Antimicrobial Chemotherapy, 2012, 67, 2110-2113.	1.3	38
108	Crystal sample pins and a storage cassette system compatible with the protein crystallography beamlines at both the Photon Factory and SPring-8. Journal of Applied Crystallography, 2012, 45, 1156-1161.	1.9	0

#	Article	IF	CITATIONS
109	Micro-crystallography comes of age. Current Opinion in Structural Biology, 2012, 22, 602-612.	2.6	144
110	Crystal structures of the state 1 conformations of the GTPâ€bound Hâ€Ras protein and its oncogenic G12V and Q61L mutants. FEBS Letters, 2012, 586, 1715-1718.	1.3	66
111	Upgrade of automated sample exchanger SPACE. Journal of Applied Crystallography, 2012, 45, 234-238.	1.9	25
112	Fine-needle capillary mounting for protein microcrystals. Journal of Applied Crystallography, 2012, 45, 785-788.	1.9	3
113	Expression, purification and preliminary X-ray crystallographic analysis of cyanobacterial biliverdin reductase. Acta Crystallographica Section F: Structural Biology Communications, 2011, 67, 313-317.	0.7	4
114	Interspecies dissemination of a novel class 1 integron carrying blaIMP-19 among Acinetobacter species in Japan. Journal of Antimicrobial Chemotherapy, 2011, 66, 2480-2483.	1.3	38
115	Critical Roles of Interactions among Switch I-preceding Residues and between Switch II and Its Neighboring α-Helix in Conformational Dynamics of the GTP-bound Ras Family Small GTPases. Journal of Biological Chemistry, 2011, 286, 15403-15412.	1.6	14
116	The Catalytic Architecture of Leukotriene C4 Synthase with Two Arginine Residues. Journal of Biological Chemistry, 2011, 286, 16392-16401.	1.6	29
117	Present status of SPring-8 macromolecular crystallography beamlines. AIP Conference Proceedings, 2010, , .	0.3	6
118	Improvement in Stability of SPring-8 Standard X-Ray Monochromators with Water-Cooled Crystals. AIP Conference Proceedings, 2010, , .	0.3	3
119	New micro-beam beamline at SPring-8, targeting at protein micro-crystallography. AIP Conference Proceedings, 2010, , .	0.3	18
120	Fully Automated Data Collection Using PAM and the Development of PAMâ^•SPACE Reversible Cassettes. , 2010, , .		2
121	Mapping of the basic aminoâ€acid residues responsible for tubulation and cellular protrusion by the EFC/Fâ€BAR domain of pacsin2/Syndapin II. FEBS Letters, 2010, 584, 1111-1118.	1.3	66
122	Crystallization and preliminary X-ray crystallographic analysis ofThermus thermophilustranscription elongation complex bound to Gfh1. Acta Crystallographica Section F: Structural Biology Communications, 2010, 66, 64-68.	0.7	4
123	Crystal structure of bacterial RNA polymerase bound with a transcription inhibitor protein. Nature, 2010, 468, 978-982.	13.7	140
124	Channeling and conformational changes in the heterotetrameric sarcosine oxidase from Corynebacterium sp. U-96. Journal of Biochemistry, 2010, 148, 491-505.	0.9	15
125	Structural Basis for Conformational Dynamics of GTP-bound Ras Protein. Journal of Biological Chemistry, 2010, 285, 22696-22705.	1.6	126
126	Structural Basis of the Catalytic Mechanism Operating in Open-Closed Conformers of Lipocalin Type Prostaglandin D Synthase. Journal of Biological Chemistry, 2009, 284, 22344-22352.	1.6	38

#	Article	IF	CITATIONS
127	Crystallization and preliminary X-ray analysis of the stress-response PPM phosphatase RsbX fromBacillus subtilis. Acta Crystallographica Section F: Structural Biology Communications, 2009, 65, 1128-1130.	0.7	1
128	Development of a shutterless continuous rotation method using an X-ray CMOS detector for protein crystallography. Journal of Applied Crystallography, 2009, 42, 1165-1175.	1.9	19
129	Process of Accumulation of Metal Ions on the Interior Surface of apo-Ferritin: Crystal Structures of a Series of apo-Ferritins Containing Variable Quantities of Pd(II) Ions. Journal of the American Chemical Society, 2009, 131, 5094-5100.	6.6	88
130	Polymerization of Phenylacetylene by Rhodium Complexes within a Discrete Space of apo-Ferritin. Journal of the American Chemical Society, 2009, 131, 6958-6960.	6.6	165
131	High-throughput crystallization-to-structure pipeline at RIKEN SPring-8 Center. Journal of Structural and Functional Genomics, 2008, 9, 21-28.	1.2	25
132	Mail-in data collection at SPring-8 protein crystallography beamlines. Journal of Synchrotron Radiation, 2008, 15, 288-291.	1.0	43
133	Crystallization and preliminary X-ray diffraction anaylsis of the LOV1 domains of phototropin 1 and 2 from <i>Arabidopsis thaliana</i> . Acta Crystallographica Section F: Structural Biology Communications, 2008, 64, 617-621.	0.7	3
134	Interaction and Stoichiometry of the Peripheral Stalk Subunits NtpE and NtpF and the N-terminal Hydrophilic Domain of Ntpl of Enterococcus hirae V-ATPase. Journal of Biological Chemistry, 2008, 283, 19422-19431.	1.6	25
135	Crystal Structures of Blasticidin S Deaminase (BSD). Journal of Biological Chemistry, 2007, 282, 37103-37111.	1.6	19
136	Beamline for Biological Macromolecular Assemblies (BL44XU) at SPring-8. AIP Conference Proceedings, 2007, , .	0.3	4
137	Curved EFC/F-BAR-Domain Dimers Are Joined End to End into a Filament for Membrane Invagination in Endocytosis. Cell, 2007, 129, 761-772.	13.5	366
138	Dose dependence of radiation damage for protein crystals studied at various X-ray energies. Journal of Synchrotron Radiation, 2007, 14, 4-10.	1.0	64
139	Preliminary X-ray crystallographic study of glucose dehydrogenase fromThermus thermophilusHB8. Acta Crystallographica Section F: Structural Biology Communications, 2007, 63, 446-448.	0.7	1
140	The 1.48 à Resolution Crystal Structure of the Homotetrameric Cytidine Deaminase from Mouse‡. Biochemistry, 2006, 45, 7825-7833.	1.2	53
141	Structure Basis for Antitumor Effect of Aplyronine A. Journal of Molecular Biology, 2006, 356, 945-954.	2.0	77
142	RIKEN structural genomics beamlines at the SPring-8; high throughput protein crystallography with automated beamline operation. Journal of Structural and Functional Genomics, 2006, 7, 15-22.	1.2	94
143	Beamline Scheduling Software: administration software for automatic operation of the RIKEN structural genomics beamlines at SPring-8. Journal of Synchrotron Radiation, 2005, 12, 380-384.	1.0	60
144	Purification, crystallization and preliminary X-ray diffraction analysis of the Kelch-like motif region of mouse Keap1. Acta Crystallographica Section F: Structural Biology Communications, 2005, 61, 153-155.	0.7	16

#	Article	IF	CITATIONS
145	Highly polarized electrons from GaAs–GaAsP and InGaAs–AlGaAs strained-layer superlattice photocathodes. Journal of Applied Physics, 2005, 97, 094907.	1.1	70
146	Crystal Structure of M-Ras Reveals a GTP-bound "Off―State Conformation of Ras Family Small GTPases. Journal of Biological Chemistry, 2005, 280, 31267-31275.	1.6	63
147	A Norovirus Protease Structure Provides Insights into Active and Substrate Binding Site Integrity. Journal of Virology, 2005, 79, 13685-13693.	1.5	70
148	Structural Basis of the Substrate-specific Two-step Catalysis of Long Chain Fatty Acyl-CoA Synthetase Dimer. Journal of Biological Chemistry, 2004, 279, 31717-31726.	1.6	189
149	Structural Basis of Leukotriene B4 12-Hydroxydehydrogenase/15-Oxo-prostaglandin 13-Reductase Catalytic Mechanism and a Possible Src Homology 3 Domain Binding Loop. Journal of Biological Chemistry, 2004, 279, 22615-22623.	1.6	58
150	Structure and implications for the thermal stability of phosphopantetheine adenylyltransferase fromThermus thermophilus. Acta Crystallographica Section D: Biological Crystallography, 2004, 60, 97-104.	2.5	28
151	A large-area CMOS imager as an X-ray detector for synchrotron radiation experiments. Journal of Synchrotron Radiation, 2004, 11, 347-352.	1.0	21
152	Sample management system for a vast amount of frozen crystals at SPring-8. Journal of Applied Crystallography, 2004, 37, 867-873.	1.9	61
153	Mechanism of metal activation of human hematopoietic prostaglandin D synthase. Nature Structural and Molecular Biology, 2003, 10, 291-296.	3.6	64
154	Cloning, Expression, Crystallization, and Preliminary X-Ray Analysis of Recombinant Mouse Lipocalin-type Prostaglandin D Synthase, a Somnogen-Producing Enzyme. Journal of Biochemistry, 2003, 133, 29-32.	0.9	20
155	Crystal Structures of 4-α-Glucanotransferase from Thermococcus litoralis and Its Complex with an Inhibitor. Journal of Biological Chemistry, 2003, 278, 19378-19386.	1.6	82
156	The Flexible C-Terminal Region of Aspergillus terreus Blasticidin S Deaminase: Identification of Its Functional Roles with Deletion Enzymes. Biochemical and Biophysical Research Communications, 2002, 290, 421-426.	1.0	4
157	Mechanism of c-Myb–C/EBPβ Cooperation from Separated Sites on a Promoter. Cell, 2002, 108, 57-70.	13.5	155
158	Crystal structure of lipocalin-type prostaglandin D synthase. International Congress Series, 2002, 1233, 453-459.	0.2	2
159	Trichromatic Concept Optimizes MAD Experiments in Synchrotron X-Ray Crystallography. Structure, 2002, 10, 1205-1210.	1.6	22
160	The 1.55 Ã resolution structure of Nicotiana alata SF11-RNase associated with gametophytic self-incompatibility. Journal of Molecular Biology, 2001, 314, 103-112.	2.0	61
161	Structural Analyses of DNA Recognition by the AML1/Runx-1 Runt Domain and Its Allosteric Control by CBFî². Cell, 2001, 104, 755-767.	13.5	317
162	Development of high-speed Imaging Plate detector. Nuclear Instruments and Methods in Physics Research, Section A: Accelerators, Spectrometers, Detectors and Associated Equipment, 2001, 467-468, 1160-1162.	0.7	7

#	Article	IF	CITATIONS
163	Structure of a new `aspzincin' metalloendopeptidase fromGrifola frondosa: implications for the catalytic mechanism and substrate specificity based on several different crystal forms. Acta Crystallographica Section D: Biological Crystallography, 2001, 57, 361-368.	2.5	36
164	Crystallization and preliminary X-ray analyses of quaternary, ternary and binary protein–DNA complexes with involvement of AML1/Runx-1/CBFα Runt domain, CBFβ and the C/EBPβ bZip region. Acta Crystallographica Section D: Biological Crystallography, 2001, 57, 850-853.	2.5	7
165	Crystals of ternary protein–DNA complexes composed of DNA-binding domains of c-Myb or v-Myb, C/EBPα or C/EBPβ andtom-1A promoter fragment. Acta Crystallographica Section D: Biological Crystallography, 2001, 57, 1655-1658.	2.5	8
166	Structure of the bacterial flagellar protofilament and implications for a switch for supercoiling. Nature, 2001, 410, 331-337.	13.7	480
167	Trichromatic Concept for Rapid Protein Crystallographic Analysis. Seibutsu Butsuri, 2001, 41, 156-159.	0.0	1
168	Reaction Mechanism and Crystal Structure of 4ALPHAGlucanotransferase from a Hyperthermophilic Archaeon, Thermococcus litoralis Journal of Applied Glycoscience (1999), 2001, 48, 171-175.	0.3	7
169	Prospects for X-ray Crystal Structure Analysis of Selenoproteins with SPring-8 Synchrotron Radiation Journal of Health Science, 2000, 46, 426-429.	0.9	0
170	X-ray Structure of β-Carbonic Anhydrase from the Red Alga,Porphyridium purpureum, Reveals a Novel Catalytic Site for CO2 Hydration. Journal of Biological Chemistry, 2000, 275, 5521-5526.	1.6	151
171	Crystallization and Preliminary X-Ray Crystallographic Studies of Thermus thermophilus HB8 MutM Protein Involved in Repairs of Oxidative DNA Damage. Journal of Biochemistry, 2000, 127, 9-11.	0.9	3
172	Small-angle X-ray scattering station at the SPring-8 RIKEN beamline. Journal of Applied Crystallography, 2000, 33, 797-800.	1.9	166
173	Structural basis of glutamate recognition by a dimeric metabotropic glutamate receptor. Nature, 2000, 407, 971-977.	13.7	1,185
174	Crystal structure of N-carbamyl-d-amino acid amidohydrolase with a novel catalytic framework common to amidohydrolases. Structure, 2000, 8, 729-738.	1.6	122
175	Crystal structure of a repair enzyme of oxidatively damaged DNA, MutM (Fpg), from an extreme thermophile,Thermus thermophilusHB8. EMBO Journal, 2000, 19, 3857-3869.	3.5	141
176	Crystal structure combined with genetic analysis of the Thermus thermophilus ribosome recycling factor shows that a flexible hinge may act as a functional switch. Rna, 2000, 6, 1432-1444.	1.6	70
177	Crystal Structure of the Pyridoxal 5'-phosphate Dependent L-Methionine Â-Lyase from Pseudomonas putida. Journal of Biochemistry, 2000, 128, 349-354.	0.9	47
178	The adoption of a twisted structure of importin-β is essential for the protein-protein interaction required for nuclear transport 1 1Edited by K. Nagai. Journal of Molecular Biology, 2000, 302, 251-264.	2.0	66
179	Crystal Structure of Rhodopsin: A G Protein-Coupled Receptor. Science, 2000, 289, 739-745.	6.0	5,486
180	A multiple CCD X-ray detector and its first operation with synchrotron radiation X-ray beam. Nuclear Instruments and Methods in Physics Research, Section A: Accelerators, Spectrometers, Detectors and Associated Equipment, 1999, 436, 174-181.	0.7	4

#	Article	IF	CITATIONS
181	A multiple-CCD X-ray detector and its basic characterization. Journal of Synchrotron Radiation, 1999, 6, 6-18.	1.0	9
182	Crystal structure of the RNA-dependent RNA polymerase of hepatitis C virus. Structure, 1999, 7, 1417-1426.	1.6	381
183	The start of a new generation: the present status of the SPring-8 synchrotron and its use in structural biology. Structure, 1999, 7, R183-R187.	1.6	5
184	Trichromatic Concept at SPring-8 RIKEN Beamline I. Journal of Synchrotron Radiation, 1998, 5, 222-225.	1.0	35
185	Standard Transport Channels of X-ray Beamlines at SPring-8. Journal of Synchrotron Radiation, 1998, 5, 1202-1205.	1.0	16
186	Evaluation of high spatial resolution imaging plate. Nuclear Instruments and Methods in Physics Research, Section A: Accelerators, Spectrometers, Detectors and Associated Equipment, 1998, 416, 314-318.	0.7	7
187	Crystal Structure of H2-Proteinase from the Venom of Trimeresurus flavoviridis. Journal of Biochemistry, 1996, 119, 49-57.	0.9	62
188	Cryocrystallography of 3-Isopropylmalate Dehydrogenase fromThermus thermophilusand its Chimeric Enzyme. Acta Crystallographica Section D: Biological Crystallography, 1996, 52, 623-630.	2.5	12
189	Crystallization and Preliminary X-Ray Study of H2-Proteinase from the Venom of Trimeresurus flavoviridis. Journal of Biochemistry, 1995, 117, 929-930.	0.9	1
190	Fundamental design of the high energy undulator pilot beamline for macromolecular crystallography at the SPringâ€8. Review of Scientific Instruments, 1995, 66, 1703-1705.	0.6	20
191	Conceptual design of SPringâ€8 contract beamline for structural biology. Review of Scientific Instruments, 1995, 66, 1833-1835.	0.6	18
192	Development of a proportional scintillation xâ€ray imaging chamber for synchrotron radiation experiments. Review of Scientific Instruments, 1995, 66, 2336-2338.	0.6	1